

NANO EXPRESS

Open Access



Telecommunication Wavelength-Band Single-Photon Emission from Single Large InAs Quantum Dots Nucleated on Low-Density Seed Quantum Dots

Ze-Sheng Chen^{1,2}, Ben Ma^{2,3}, Xiang-Jun Shang^{2,3}, Yu He^{3,4}, Li-Chun Zhang^{2,3}, Hai-Qiao Ni^{2,3}, Jin-Liang Wang¹ and Zhi-Chuan Niu^{2,3*}

Abstract

Single-photon emission in the telecommunication wavelength band is realized with self-assembled strain-coupled bilayer InAs quantum dots (QDs) embedded in a planar microcavity on GaAs substrate. Low-density large QDs in the upper layer active for $\sim 1.3 \mu\text{m}$ emission are fabricated by precisely controlling the indium deposition amount and applying a gradient indium flux in both QD layers. Time-resolved photoluminescence (PL) intensity suggested that the radiative lifetime of their exciton emission is 1.5–1.6 ns. The second-order correlation function of $g^2(0) < 0.5$ which demonstrates a pure single-photon emission.

Keywords: Bilayer quantum dot, Telecommunication wavelength, Single-photon source

Abbreviations: QD, Quantum dot; PL, Photoluminescence; θ_c , Critical coverage; SPS, Single-photon sources; DBRs, Distributed Bragg reflectors; DWELL, Dot-in-well; BQD, Bilayer quantum dot; SNSPD, Superconducting nanowire single-photon detector; AFM, Atomic force microscope; HBT, Hanbury-Brown-Twiss; MBE, Molecular beam epitaxy; SQD, Sacrificed InAs quantum dot; RHEED, Reflection high-energy electron-diffraction; SRL, Strain-reducing layer; μPL , Micro-PL; TCSPC, Time-correlated single photon counting; FWHM, Full width at half maximum

Background

Real single-photon sources (SPSs) at telecommunication wavelength are very important for optical fiber-based quantum information that is practical for security application [1–3]. Semiconductor single quantum dots (QDs) are the best candidates to emit true single photons. In recent decades, InAs QDs [4, 5] have attracted great interest in quantum information [6, 7] and quantum computation [8]. Being compatible with GaAs/Al(Ga)As distributed Bragg reflectors (DBRs) to form a planar microcavity to enhance QD emission, GaAs-based InAs QDs have demonstrated high-intensity single-photon

emission in wavelength $< 1000 \text{ nm}$ [9]. However, it is difficult to obtain $1.3 \mu\text{m}$ or longer-wavelength single-photon emission on them, which was limited by QD material itself. Although InAs/InP QDs can emit single photons in a $1.55\text{-}\mu\text{m}$ wavelength range [10, 11], it is difficult to combine them with a high-Q DBR cavity. To extend the emission wavelength of InAs/GaAs QDs to telecommunication wavelength, several methods have been developed, such as asymmetric InGaAs/GaAs dot-in-well (DWELL) structure [12], 30 % In-content InGaAs capping layer [13], strain engineering of QDs [14], metamorphic structures [15], and vertically coupled QDs, i.e., bilayer QDs (BQDs) [16–18] where active QDs are formed on seed QDs capped with InGaAs. The BQD structure is advantageous on the growth since their growth parameters, such as growth rate, spacer layer thickness, indium deposition amount, and growth temperature can be precisely controlled. High-density BQDs have been grown to

* Correspondence: zcnui@semi.ac.cn

²State Key Laboratory for Superlattices and Microstructures, Institute of Semiconductors, Chinese Academy of Science, Beijing 100083, China

³Hefei National Laboratory for Physical Sciences at Microscale and Department of Modern Physics, University of Science and Technology of China, Hefei, Anhui 230026, China

Full list of author information is available at the end of the article

realize laser diodes at $\sim 1.5 \mu\text{m}$ [17, 19]. However, few reports have forced on the growth of low-density BQDs for telecommunication-band single-photon emission. In fact, to realize low-density BQDs, the density and distribution of both the seed QDs and the active QDs and their inter-layer strain coupling must be well controlled, which is more difficult than the growth of the traditional single-layer low-density QDs in wavelength $< 1000 \text{ nm}$.

In this paper, low-density active QDs with emission wavelength at $1.3 \mu\text{m}$ are realized on low-density seed QDs by well utilizing the interlayer strain coupling and precisely controlling the gradient indium deposition amount in seed QD layer and active QD layer on a non-rotating substrate. These BQDs are embedded inside a GaAs $1\text{-}\lambda$ cavity in the DBR structure to enhance QD emission in the normal direction. The second-order correlation function measurement demonstrates nice single-photon emission. This is the first time to apply this material system on telecommunication-band single-photon emission. The emission intensity of such single QDs could be improved by optimizing the growth parameters, e.g., the growth temperature of QDs.

Methods

The samples were grown by solid source molecular beam epitaxy (MBE; VEECO Gen930 system) on semi-insulating (100) GaAs substrates. The structure of sample A is shown in Fig. 1a. After a 300-nm-thick GaAs buffer layer growth at $580 \text{ }^\circ\text{C}$, a planar $1\text{-}\lambda$ GaAs micro-cavity sandwiched between 20.5 pairs of the bottom and

eight pairs of the top $\text{Al}_{0.9}\text{Ga}_{0.1}\text{As}$ (113.7 nm)/GaAs (98.6 nm) DBR was grown, whose quality factor (Q), as characterized later, is ≈ 200 . The integration into the DBR cavity increases the extraction efficiency of photon emission from a single active QD. In fact, without DBR, there is no micro-photoluminescence (μPL) signal detected in our experiment. The BQD structure capped with $5 \text{ nm In}_{0.15}\text{Ga}_{0.85}\text{As}$ was embedded at the cavity antinode to maximize the cavity enhancement [17, 20, 21]. The QD growth is detailed as follows: on the 80-nm GaAs above the bottom DBR, a sacrificed InAs quantum dot (SQD) layer was deposited at $540 \text{ }^\circ\text{C}$ by using a very low growth rate of 0.005 ML s^{-1} and a periodic growth method with a 5-s interruption after each 20-s deposition of indium, under As_2 -stabilized condition. The critical coverage (θ_c) for island formation was monitored by reflection high-energy electron-diffraction (RHEED). As RHEED monitored, the θ_c was 2.2 ML. After it, the SQD growth was stopped immediately and the substrate was annealed at $670 \text{ }^\circ\text{C}$ for 10 min to desorb SQDs completely [22]. Then, a 108.6-nm GaAs was deposited at $580 \text{ }^\circ\text{C}$ and the substrate temperature was cooled down to $540 \text{ }^\circ\text{C}$ to grow seed QDs. The substrate rotation was stopped to build a gradient indium flux on the substrate and form density-graded seed QDs. The growth rate and deposition method is the same as that of SQDs but with a sub- θ_c indium coverage. After 5 s of growth interruption, the GaAs spacer was grown at $540 \text{ }^\circ\text{C}$ immediately. It was in moderate thickness (i.e., 8 nm), allowing a capping of seed QDs and a residual strain field on them (as nucleation sites) in favor

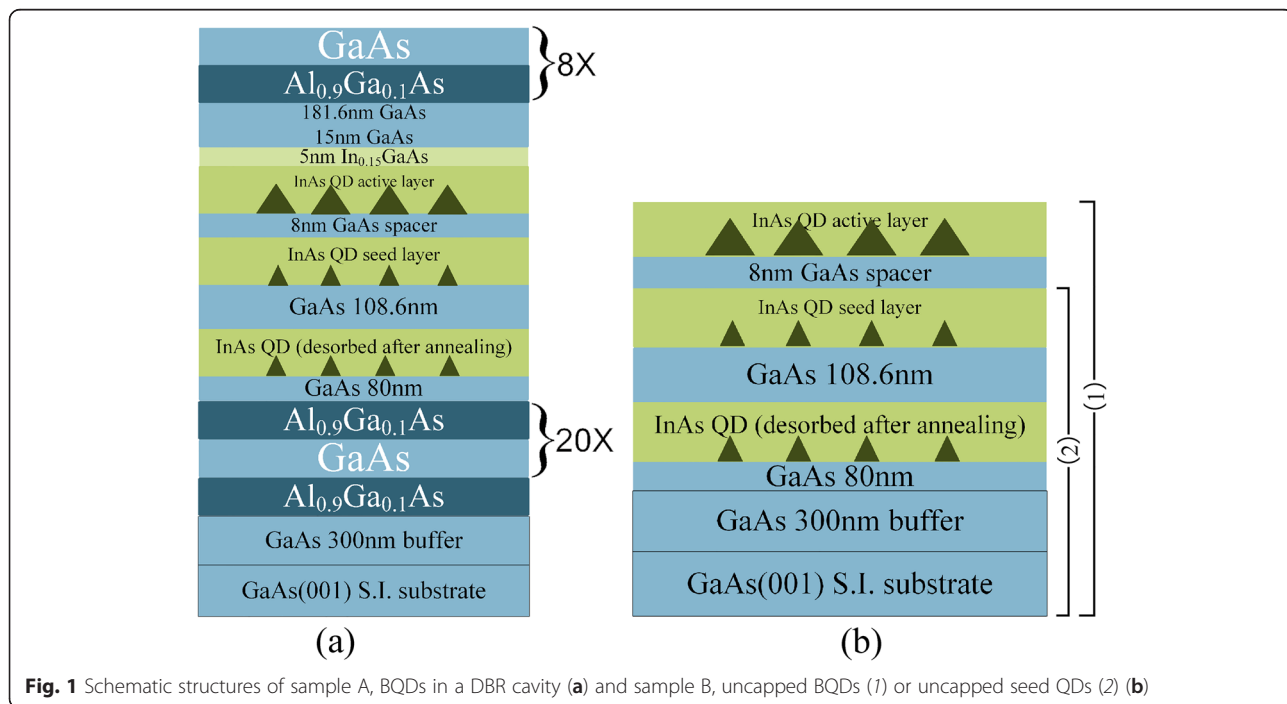
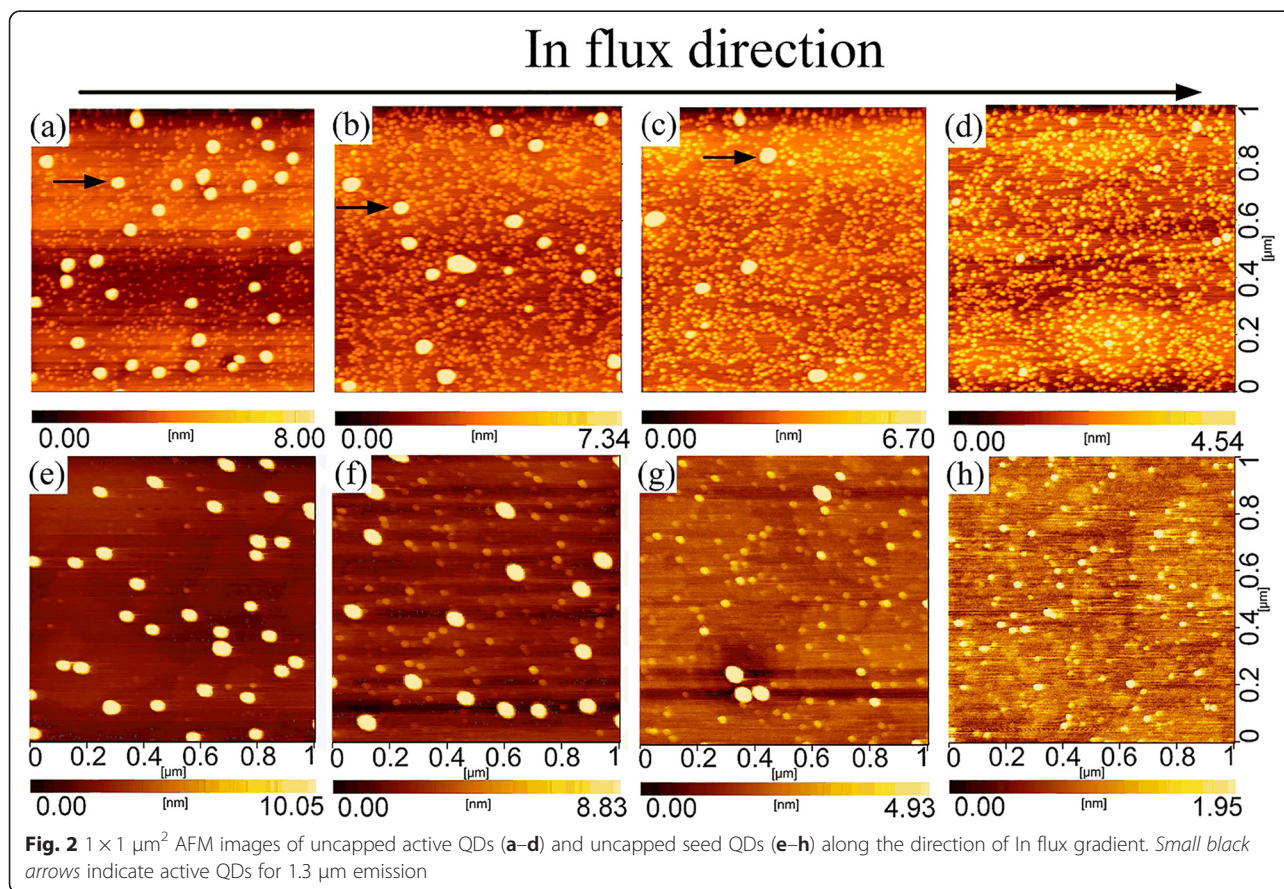


Fig. 1 Schematic structures of sample A, BQDs in a DBR cavity (a) and sample B, uncapped BQDs (1) or uncapped seed QDs (2) (b)

of vertically aligned active QD formation [20, 23]. A subsequent annealing at 610 °C for 10 min was used to remove the intrinsic defects and flattening the surface [18, 24–26] before deposition of the second QD layer. The substrate temperature was cooled down to 480 °C, and 2.0 ML of InAs coverage was deposited in a growth rate of 0.02 ML s⁻¹ to form the active QDs. After a 5-s growth interruption, a 5-nm In_{0.15}Ga_{0.85}As strain-reducing layer (SRL) [20] was grown immediately to maintain QD height for longer-wavelength QD emission [23, 24]. The high substrate temperature and low growth rate of seed QDs increase the migration of indium atoms to form low-density islands [16, 27, 28], while the relatively lower substrate temperature and higher growth rate for active QDs reduce their migration and intermixing with Ga and enable a prior and rapid nucleation of single large QDs on seed QDs driven by strain, in a high optical quality [24, 29–31]. On the SRL, a 15-nm GaAs was capped in the same temperature and the rotation of substrate was resumed for the following steps. Finally, the substrate temperature raised to 580 °C to grow the top 181.6-nm GaAs and the top eight pairs of DBR. Sample A with the full cavity structure was used for optical measurements. As shown in Fig. 1b, sample B (reference sample) with uncapped BQDs (1), or uncapped seed

QDs (2), grown in the same condition but with a θ_c indium coverage in seed QD layer, was used for morphology in atomic force microscopy (AFM). μ PL spectroscopy was performed using the confocal microscopy technique with fiber-coupled input and output, excited by a 632.8-nm He-Ne laser, and detected by a liquid nitrogen-cooled CCD detector in the spectrometer. A high numerical aperture objective ($\times 100$, NA = 0.55) focuses the laser on the sample, in a diameter of ~ 2 μ m, and enables an effective collection of QD luminescence in this micro-region. The spectral line of single QD emission was filtered for further measurement. Time-resolved PL measurement used a pulsed semiconductor laser (λ 780 nm, repetition rate 80 MHz, pulse width 3 ps, power 3.6 μ W) as excitation, multi-channel superconducting nanowire single-photon detectors (SNSPD; time resolution 120 ps) for detection, and a Hydra Harp 400 module for time-correlated single photon counting (TCSPC), to investigate the radiative lifetime of the spectral line. To check its single-photon property, the second-order correlation measurement was done in Hanbury-Brown-Twiss (HBT) scheme [27, 32–34] by splitting the signal into two parts with a 50:50 beam splitter in free space and detecting them with two channels of SNSPD separately in fiber coupling, and analyzing the coincidence of both SNSPD outputs with TCSPC.



Results and Discussion

Figure 2a–d shows the AFM images of active QDs along the direction of In flux gradient. Figure 2e–h shows the AFM images of seed QDs, correspondingly. The gradient In flux formed density-graded large QDs [35], among dense small QDs, i.e., bimodal QD size distribution. As In deposition amount decreases along the In flux direction, the large QDs evolve from high density ($\sim 3.5 \times 10^9 \text{ cm}^{-2}$ in Fig. 2a and $\sim 1.8 \times 10^9 \text{ cm}^{-2}$ in Fig. 2b) to low density ($\sim 6 \times 10^8 \text{ cm}^{-2}$ in Fig. 2c), and finally no large QDs

(Fig. 2d). In contrast, the density of small QDs in active QD layer increased as the indium deposition decreases, from about $8.8 \times 10^{10} \text{ cm}^{-2}$ in Fig. 2a to $\sim 1.4 \times 10^{11}$, $\sim 1.7 \times 10^{11}$, and $\sim 2 \times 10^{11} \text{ cm}^{-2}$ in Fig. 2b–d, respectively. It reflects the collection of small QDs into a larger one during QD growth. In seed QD layer, the density of small QDs is much lower; the density of large QDs reduces from $3.4 \times 10^9 \text{ cm}^{-2}$ in Fig. 2e to 1.8×10^9 , $4 \times 10^8 \text{ cm}^{-2}$, and zero in Fig. 2f–h, respectively, similar to the large QDs in the active QD layer. It suggests that the large active QDs

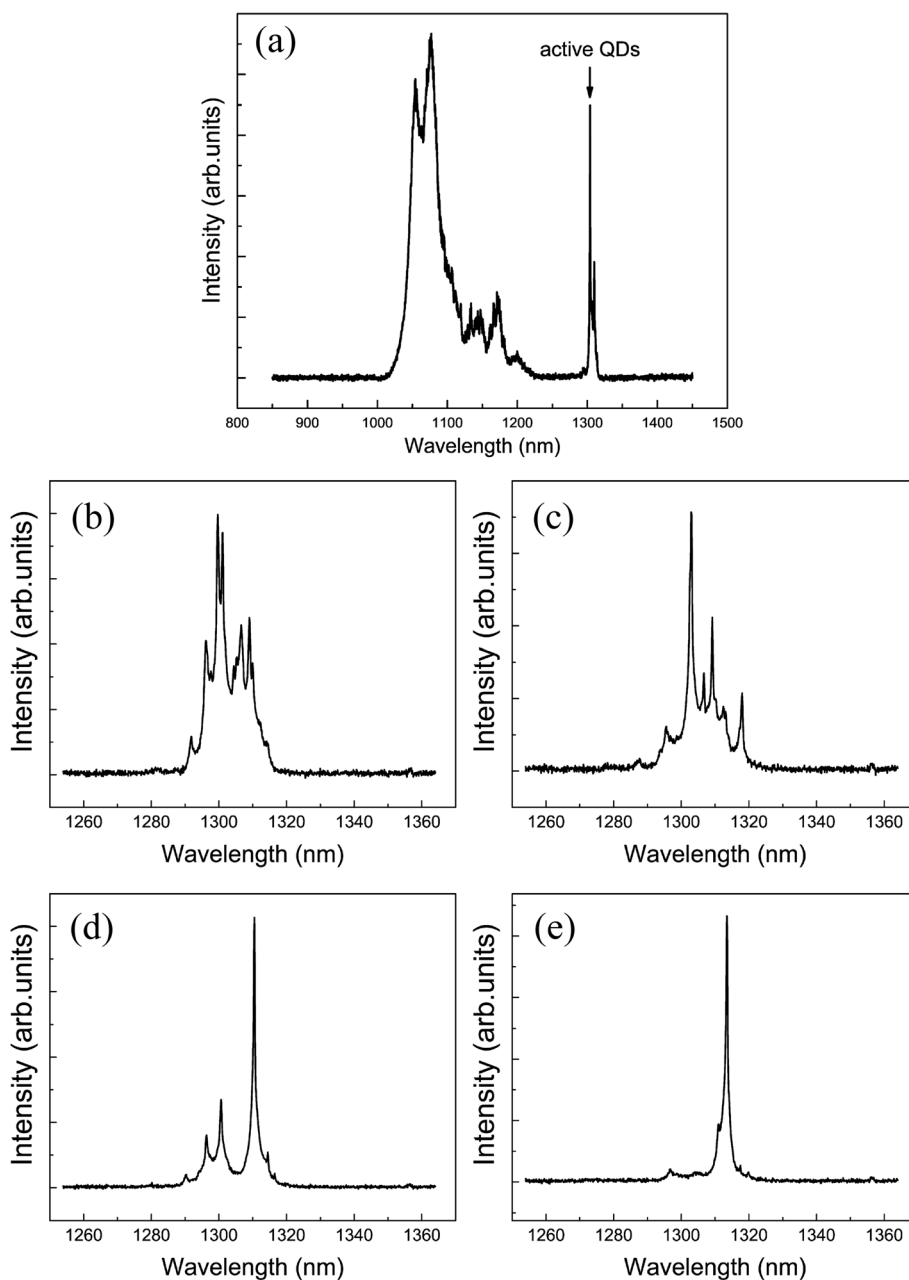


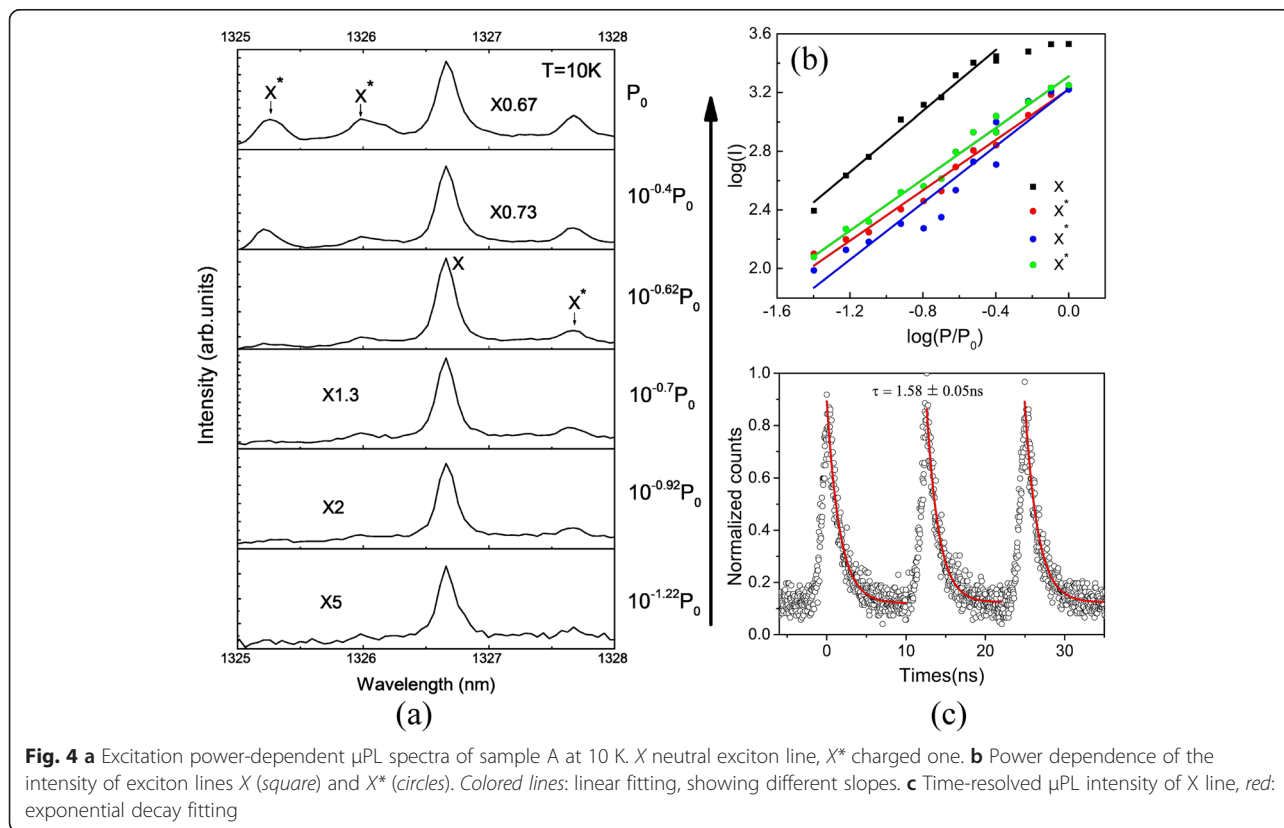
Fig. 3 μ PL spectra of sample A at 80 K. **a** Full spectrum. **b–e** Along the direction of In flux gradient

are grown on the large seed QDs whose strain field is strong enough to build nucleation sites, enabling a prior QD nucleation, while the dense small QDs in the active layer nucleate due to the low growth temperature and high growth rate that reduced surface diffusion of In atoms [36]. Therefore, the gradient In flux is an efficient way to get low-density BQDs. However, their density is still too high to realize a single QD in a micro-region for single-photon emission. So, in sample A for optical measurement, a sub- θ_c indium coverage in seed layer was used to reduce the density of active QDs.

Figure 3 presents the μ PL spectra of sample A along the In flux gradient direction. The sample was cooled at 80 K. In Fig. 3a, some weak and broad peaks appear between 1020 and 1200 nm, which are from QDs in the seed layer and the small QDs in the active layer [14, 37]; the $\sim 1.3\text{-}\mu\text{m}$ emission comes from active large QDs. The trend of μ PL spectra is well consistent with that of AFM images in Fig. 2. In Fig. 3b, c, the μ PL spectra are envelope profiles, corresponding to high-density active QDs. The multiple peaks in Fig. 3d demonstrate an obvious decreasing of the density of active QDs. In Fig. 3e, the sharp single spectral line suggests single QD formation. The big variation of large QD density and their μ PL spectra along the In flux direction suggests that QD formation is very sensitive on the indium coverage. On the

other hand, the gradient In flux method ensures a high-repeatability of low-density large QD formation.

To further characterize the spectral lines like in Fig. 3e, power-dependent μ PL spectroscopy was performed at 10 K in a cryogen-free bath cryostat [38], as shown in Fig. 4a. The spectrum is dominated by the emission of the X exciton at an emission wavelength of 1326.7 nm. At low excitation power, only the X line appeared, in a narrow full width at half maximum (FWHM) of 111 μeV , limited by the resolution of the measurement system and the spectral diffusion from small QDs [2, 3, 39]. By further increasing the excitation power, several other lines appeared, recognized as X and X^* exciton lines [40]. As shown in Fig. 4b, the X line at 1326.7 nm showed a near linear dependence on the excitation power (slope = 1.04). The peaks at 1325.3, 1326, and 1327.7 nm, whose power dependence showed slopes of 0.86, 0.88, and 0.97, respectively, and non-saturation under high-power excitation, came from either charged exciton or exciton recombination in neighboring less efficient QDs; they are named as X^* . We used a 80-MHz pulsed semiconductor laser to measure the lifetime of exciton X. In Fig. 4c, three peaks were chosen from the 100-ns time window to show the decay dynamics of a single exciton emission. Acquired from exponential fitting, its emission lifetime is 1.58 ± 0.05 ns on average, typical for the radiative



lifetimes of exciton recombination in InAs/GaAs QDs at telecommunication wavelength [1, 41–43].

In order to gain insight into the photon statistics of the active QD emission from the BQD material system (i.e., the spectral line in the inset of Fig. 5), we measured the second-order time correlation function $g^{(2)}(\tau)$ with a HBT setup under continuous-wave excitation. In order to accumulate the single channel counts in limited time, the time resolution was decreased in the experiment. The correlation dip at zero time delay in Fig. 5 provides evidence of antibunching (i.e., quantum) behavior of the light emission from a large InAs/GaAs QD. The solid curve in red is the fit to the data with the commonly accepted formula [44]. The antibunching dip below 0.5 suggests single-photon emission from single active QD. All the above results prove that the combination of a subcritical InAs coverage and a gradual variation of indium flux is convenient and efficient to obtain low-density and high-quality active QDs from the BQD structure in telecommunication band.

Conclusions

In summary, MBE growth of low-density active QDs is achieved by using a subcritical InAs deposition technology in seed layer and gradual variation of the indium flux. The AFM results show clear transitions from high-density active QDs to low-density ones. As confirmed by μ PL spectroscopy, single active QD was obtained at telecommunication wavelength in the low-density region. Its emission lifetime is about 1.5 ns. The power-dependent μ PL spectra suggest single exciton states. The second-order autocorrelation measurement with SNSPD yielded $g^{(2)}(\tau = 0) < 0.5$, demonstrating single-photon emission. In our later experiment, the brightness of single active QD can be well improved by

optimizing the growth parameter, i.e., such as growth temperature in active layer. As a novel material system potential for single-photon source in telecommunication wavelength, BQDs are expected to be further optimized for high-efficient emission.

Acknowledgements

The authors are grateful to Chao-yang Lu, Jian-wei Pan, Yu He, Jin-peng Li, Hui Wang, Jian Qin, Can Wang, Bi-ying Wang, Hua-lei Yin, Bao-quan Sun, and Yong-zhou Xue for their experimental support. This work is supported by the National Key Basic Research Program of China (Grant No. 2013CB933304), the National Natural Science Foundation of China (Grant No. 91321313, 61505196) and Strategic Priority Research Program B of Chinese Academy of Sciences (Grant No. XDB01010200), and China Postdoctoral Science Foundation-funded project (No. 2014M561029), and Beijing Key Discipline Fundation of Condensed Matter Physics.

Authors' Contributions

Z-SC and BM contributed equally to this work. Z-SC grew the samples; carried out the alignment and took part in discussions and in the interpretation of the result; and wrote the manuscript. X-JS and BM participated in the design of the study and discussions of the results. YH helped in the technical support for the characterizations and the reconstruction of the data. X-JS, J-LW, and L-CZ have supervised the writing of the manuscript. H-QN and Z-CN supervised the writing of the manuscript and the experimental part. All the authors have read and approved the final manuscript.

Competing Interests

The authors declare that they have no competing interests.

Author details

¹School of Physics and Nuclear Energy Engineering, Beihang University, Beijing 100191, China. ²State Key Laboratory for Superlattices and Microstructures, Institute of Semiconductors, Chinese Academy of Science, Beijing 100083, China. ³Hefei National Laboratory for Physical Sciences at Microscale and Department of Modern Physics, University of Science and Technology of China, Hefei, Anhui 230026, China. ⁴CAS Center for Excellence and Synergetic Innovation Center in Quantum Information and Quantum Physics, University of Science and Technology of China, Hefei, Anhui 230026, China.

Received: 10 March 2016 Accepted: 20 August 2016

Published online: 30 August 2016

References

- Xu XL, Brossard F, Hammura K, Williams DA, Alloing B, Li LH, Fiore A (2008) "Plug and play" single photons at 1.3 μ m approaching gigahertz operation. *Appl Phys Lett* 93:021124
- Ward MB, Karimov OZ, Unitt DC, Yuan ZL, See P, Gevaux DG, Shields AJ, Atkinson P, Ritchie DA (2005) On-demand single-photon source for 1.3 μ m telecom fiber. *Appl Phys Lett* 86:201111
- Zinoni C, Alloing B, Monat C, Zwiller V, Li LH, Fiore A, Lunghi L, Gerardino A, de Riedmatten H, Zbinden H, Gisin N (2006) Time-resolved and antibunching experiments on single quantum dots at 1300 nm. *Appl Phys Lett* 88:131102
- Karrai K, Warburton RJ, Schulhauser C, Hogeleg A, Urbaszek B, McGhee EJ, Govorov AO, Garcia JM, Gerardot BD, Petroff PM (2004) Hybridization of electronic states in quantum dots through photon emission. *Nature* 427: 135–138
- Thompson RM, Stevenson RM, Shields AJ, Farrer I, Lobo CJ, Ritchie DA, Leadbeater ML, Pepper M (2001) Single-photon emission from exciton complexes in individual quantum dots. *Phys Rev B* 64:201302
- Bouwmeester D, Ekert A, Zeilinger A (2000) *The physics of quantum information*. Vol. 3. Springer, Berlin
- Gisin N, Ribordy G, Tittel W, Zbinden H (2002) Quantum cryptography. *Rev Mod Phys* 74:145–195
- Bennett CH (1992) Quantum cryptography using any two nonorthogonal states. *Phys Rev Lett* 68:3121–3124
- Schleehahn A, Gaafar M, Vaupel M, Gschrey M, Schnauber P, Schulze JH, Rodt S, Strittmatter A, Stolz W, Rahimi-Iman A (2015) Single-photon emission at a rate of 143 MHz from a deterministic quantum-dot microlens triggered by a

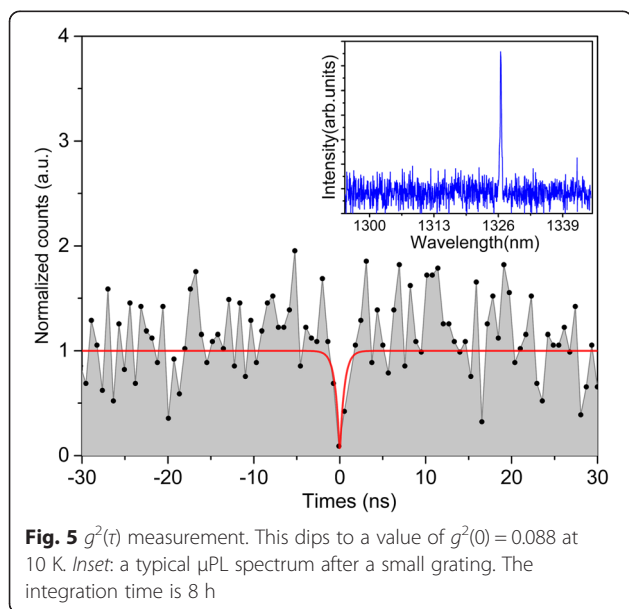


Fig. 5 $g^{(2)}(\tau)$ measurement. This dips to a value of $g^{(2)}(0) = 0.088$ at 10 K. Inset: a typical μ PL spectrum after a small grating. The integration time is 8 h

- mode-locked vertical-external-cavity surface-emitting laser. *Appl Phys Lett* 107:041105
10. Kazuya T, Yoshiki S, Shinichi H, Tatsuya U, Naoki Y, Toshiyuki M, Motomu T, Yasuhiko A (2004) Non-classical photon emission from a single InAs/InP quantum dot in the 1.3- μm optical-fiber band. *Jpn J Appl Phys* 43:L993
 11. Liu XM, Ha N, Nakajima H, Mano T, Kuroda T, Urbaszek B, Kumano H, Suemune I, Sakuma Y, Sakoda K (2014) Vanishing fine-structure splittings in telecommunication-wavelength quantum dots grown on (111) A surfaces by droplet epitaxy. *Phys Rev B* 90:081301
 12. Zhang Z, Oehler A, Resan B, Kurmulis S, Zhou K, Wang Q, Mangold M, Südmeyer T, Keller U, Weingarten K (2012) 1.55 μm InAs/GaAs quantum dots and high repetition rate quantum dot SESAM mode-locked laser. *Scientific reports* 2:477
 13. Seravalli L, Frigeri P, Minelli M, Allegri P, Avanzini V, Franchi S (2005) Quantum dot strain engineering for light emission at 1.3, 1.4 and 1.5 μm . *Appl Phys Lett* 87:063101
 14. Shimomura K, Kamiya I (2015) Strain engineering of quantum dots for long wavelength emission: photoluminescence from self-assembled InAs quantum dots grown on GaAs (001) at wavelengths over 1.55 μm . *Appl Phys Lett* 106:082103
 15. Seravalli L, Trevisi G, Frigeri P, Rivas D, Munoz-Matutano G, Suárez I, Alén B, Canet-Ferrer J, Martínez-Pastor J (2011) Single quantum dot emission at telecom wavelengths from metamorphic InAs/InGaAs nanostructures grown on GaAs substrates. *Appl Phys Lett* 98:173112
 16. Clarke E, Howe P, Taylor M, Spencer P, Harbord E, Murray R, Kadkhodazadeh S, McComb D, Stevens B, Hogg R (2010) Persistent template effect in InAs/GaAs quantum dot bilayers. *J Appl Phys* 107:113502
 17. Majid MA, Childs DT, Shahid H, Chen S, Kennedy K, Airey RJ, Hogg R, Clarke E, Howe P, Spencer PD (2011) Toward 1550-nm GaAs-based lasers using InAs/GaAs quantum dot bilayers. *Selected Topics in Quantum Electronics, IEEE Journal of* 17:1334–1342
 18. Le Ru EC, Bennett AJ, Roberts C, Murray R (2002) Strain and electronic interactions in InAs/GaAs quantum dot multilayers for 1300 nm emission. *J Appl Phys* 91:1365–1370
 19. Clarke E, Spencer P, Harbord E, Howe P, Murray R (2008) Growth, optical properties and device characterisation of InAs/GaAs quantum dot bilayers. *J Phys Conf Ser* 107:012003
 20. Ngo C, Yoon S, Tanoto H, Hui H, Lim D, Wong V, Chua S (2011) Structural and optical properties of InAs bilayer quantum dots grown at constant growth rate and temperature. *J Cryst Growth* 323:167–171
 21. Sengupta S, Shah S, Halder N, Chakrabarti S (2010) Comparison of single-layer and bilayer InAs/GaAs quantum dots with a higher InAs coverage. *Opto-Electronics Review* 18:295–299
 22. Li MF, Yu Y, He JF, Wang LJ, Zhu Y, Shang XJ, Ni HQ, Niu ZC (2013) In situ accurate control of 2D-3D transition parameters for growth of low-density InAs/GaAs self-assembled quantum dots. *Nanoscale Res Lett* 8:1–6
 23. Mukhametzhanov I, Heitz R, Zeng J, Chen P, Madhukar A (1998) Independent manipulation of density and size of stress-driven self-assembled quantum dots. *Appl Phys Lett* 73:1841–1843
 24. Le Ru EC, Howe P, Jones TS, Murray R (2003) Strain-engineered InAs/GaAs quantum dots for long-wavelength emission. *Phys Rev B* 67:165303
 25. Sengupta S, Shah S, Ghosh K, Halder N, Chakrabarti S (2011) Investigation of the effect of larger monolayer coverage in the active layer of bilayer InAs/GaAs quantum-dot structure and effects of post-growth annealing. *Applied Physics A* 103:245–250
 26. Joyce PB, Le Ru EC, Krzyzewski TJ, Bell GR, Murray R, Jones TS (2002) Optical properties of bilayer InAs/GaAs quantum dot structures: Influence of strain and surface morphology. *Phys Rev B* 66:075316
 27. Yu Y, Li MF, He JF, Zhu Y, Wang LJ, Ni HQ, He ZH, Niu ZC (2012) Photoluminescence study of low density InAs quantum clusters grown by molecular beam epitaxy. *Nanotechnology* 23:065706
 28. Huang SS, Niu ZC, Ni HQ, Xiong YH, Zhan F, Fang ZD, Xia JB (2007) Fabrication of ultra-low density and long-wavelength emission InAs quantum dots. *J Cryst Growth* 301–302:751–754
 29. Liang BL, Wang ZM, Mazur YI, Strelchuck VV, Salamo GJ (2006) Growth and characterization of bilayer InAs/GaAs quantum dot structures. *physica status solidi (a)* 203:2403–2410
 30. Yamaguchi K, Yujobo K, Kaizu T (2000) Stranski-Krastanov growth of InAs quantum dots with narrow size distribution. *Jpn J Appl Phys* 39:L1245
 31. Zetian M, Bhattacharya P (2005) Molecular-beam epitaxial growth and characteristics of highly uniform InAs/GaAs quantum dot layers. *J Appl Phys* 98:023510–023510.5
 32. Hafenbrak R, Ulrich SM, Michler P, Wang L, Rastelli A, Schmidt OG (2007) Triggered polarization-entangled photon pairs from a single quantum dot up to 30 K. *New J Phys* 9:315
 33. Dou XM, Sun BQ, Wang BR, Ma SS, Zhou R, Huang SS, Ni HQ, Niu ZC (2008) Tuning photoluminescence energy and fine structure splitting in single quantum dots by uniaxial stress. *Chin Phys Lett* 25:1120
 34. Hanbury Brown R, Twiss RQ (1956) A test of a new type of stellar interferometer on Sirius. *Nature* 178:1046–1048
 35. Moskalenko ES, Karlsson FK, Donchev VT, Holtz PO, Monemar B, Schoenfeld WW, Petroff PM (2005) Effects of separate carrier generation on the emission properties of InAs/GaAs quantum dots. *Nano Lett* 5:2117–2122
 36. Howe P, Le Ru EC, Clarke E, Abbey B, Murray R, Jones TS (2004) Competition between strain-induced and temperature-controlled nucleation of InAs/GaAs quantum dots. *J Appl Phys* 95:2998–3004
 37. Yu Y, Shang X-J, Li M-F, Zha G-W, Xu J-X, Wang L-J, Wang G-W, Ni H-Q, Dou X, Sun B, Niu Z-C (2013) Single InAs quantum dot coupled to different “environments” in one wafer for quantum photonics. *Appl Phys Lett* 102:201103
 38. He Y, He YM, Liu J, Wei YJ, Ramirez H, Atatüre M, Schneider C, Kamp M, Höfling S, Lu CY (2014) Dynamically controlled resonance fluorescence from a doubly dressed solid-state single emitter. *arXiv preprint arXiv:1411.6076*
 39. Patton B, Langbein W, Woggon U (2003) Trion, biexciton, and exciton dynamics in single self-assembled CdSe quantum dots. *Phys Rev B* 68:125316
 40. Shah S, Halder N, Sengupta S, Chakrabarti S (2012) Comparison of luminescence properties of bilayer and multilayer InAs/GaAs quantum dots. *Mater Res Bull* 47:130–134
 41. Xu XL, Williams DA, Cleaver JRA (2004) Electrically pumped single-photon sources in lateral p-i-n junctions. *Appl Phys Lett* 85:3238–3240
 42. Fiore A, Zinoni C, Alloing B, Monat C, Balet L, Li LH, Thomas NL, Houdr R, Lughli L, Francardi M, Gerardino A, Patriarche G (2007) Telecom-wavelength single-photon sources for quantum communications. *J Phys Condens Matter* 19:225005
 43. Miyazawa T, Nakaoka T, Usuki T, Arakawa Y, Takemoto K, Hirose S, Okumura S, Takatsu M, Yokoyama N (2008) Exciton dynamics in current-injected single quantum dot at 1.55 μm . *Appl Phys Lett* 92:161104
 44. Birowosuto MD, Sumikura H, Matsuo S, Taniyama H, van Veldhoven PJ, Nötzel R, Notomi M (2012) Fast Purcell-enhanced single photon source in 1,550-nm telecom band from a resonant quantum dot-cavity coupling. *Scientific Reports* 2:321

Submit your manuscript to a SpringerOpen[®] journal and benefit from:

- Convenient online submission
- Rigorous peer review
- Immediate publication on acceptance
- Open access: articles freely available online
- High visibility within the field
- Retaining the copyright to your article

Submit your next manuscript at ► springeropen.com